Supplementary Data

A Highly Selective and Sensitive Ratiometric Chemodosimeter for Hg^{2+} Ion Based on an Iridium(III) Complex via Thioacetal Deprotection Reaction

Fengniu Lu,[a] Masaki Yamamura[a,b] and Tatsuya Nabeshima[a,b,*]

[a] *Graduate School of Pure and Applied Sciences, University of Tsukuba, Tsukuba, Ibaraki 305-8571, Japan*
[b] *Tsukuba Research Center for Interdisciplinary Materials Science (TIMS), University of Tsukuba, Tsukuba, Ibaraki 30-8571, Japan*

E-mail: nabesima@chem.tsukuba.ac.jp

Table of Contents

1. Spectroscopic data of Ir-S and Ir-CHO

Table S1. Absorption and photophysical data of **Ir-S** and **Ir-CHO** (5 μM), 298 K, λ_{ex} = 400 nm.

Compound	Solvent	Absorption feature, nm[a] (ε, 10^4 dm^3 mol^{-1} cm^{-1})	Luminescence		
			λ_{max}[a], nm	Φ[a]	Φ[b]
Ir-S	CH_3CN	261(4.60), 298(2.70), 381(0.45), 411(0.34)	590	0.068	0.280
	CH_2Cl_2	258(4.80), 267 (4.65), 368(0.58), 412(0.39)	585	—	—
Ir-CHO	CH_3CN	271(4.53), 298(3.96), 364(0.57), 420(0.40)	540	0.037	0.459
	CH_2Cl_2	273(4.85), 299(4.06), 367(0.67), 418(0.46)	534	—	—

[a] In air equilibrated acetonitrile. [b] In deaerated acetonitrile.

2. Absorption and emission spectra of Ir-S and Ir-CHO in CH_3CN and CH_2Cl_2

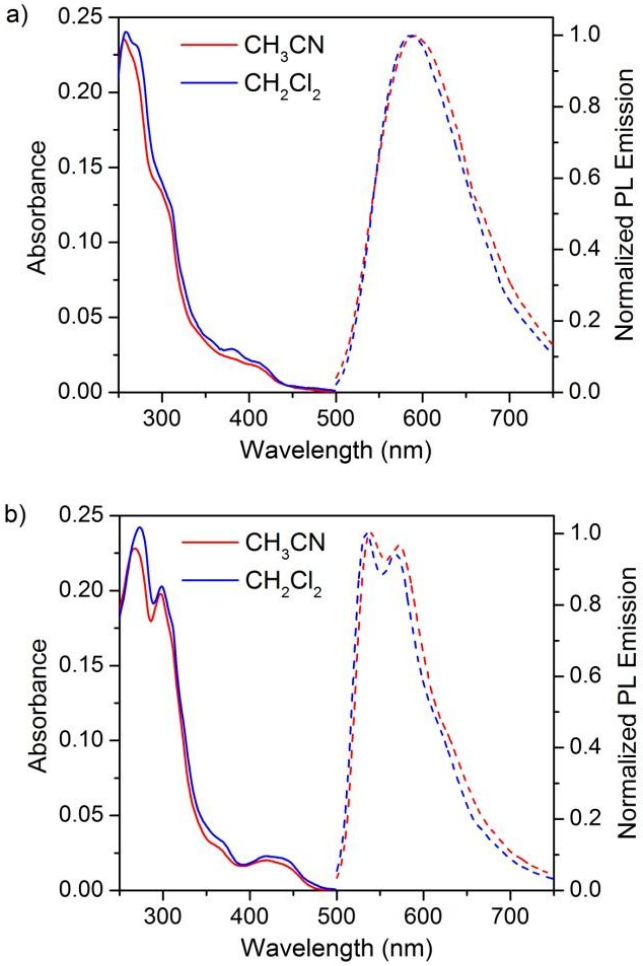

Figure S1. The UV-vis absorption (solid lines) and PL emission spectra (dash lines) of a) **Ir-S** (5 μM) and b) **Ir-CHO** (5 μM) in CH_3CN (red) and CH_2Cl_2 (blue). λ_{ex} = 400 nm.

3. Influence of water on the emission of Ir-S and Ir-CHO

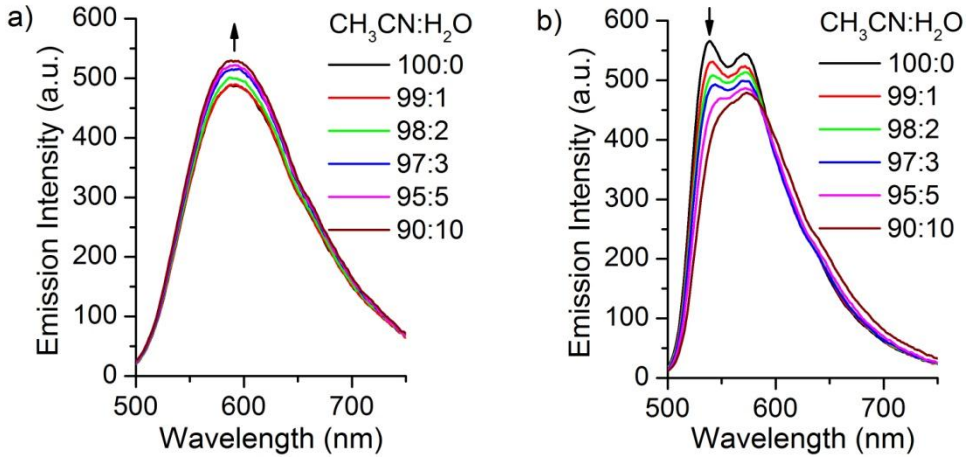

Figure S2. The emission spectra of a) **Ir-S** (5 μM) and b) **Ir-CHO** (5 μM) in different CH_3CN-H_2O solvent systems. λ_{ex} = 420 nm.

4. Time dependence of the response of Ir-S to Hg^{2+} in different solvent systems

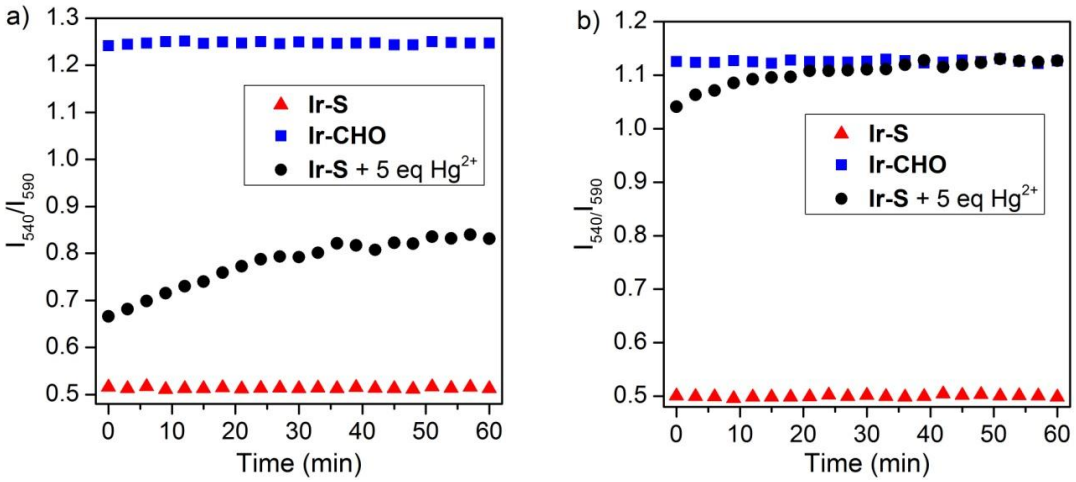

Fig. S3 Effect of time on the emission intensity ratio I_{540}/I_{590} of **Ir-CHO** (5 μM) and **Ir-S** (5 μM) in the absence and presence of 5 equiv. Hg^{2+} in a) CH_3CN and b) CH_3CN/H_2O (98/2, v/v). λ_{ex} = 420 nm.

5. Absorption spectral changes of Ir-S upon titration of Hg^{2+}

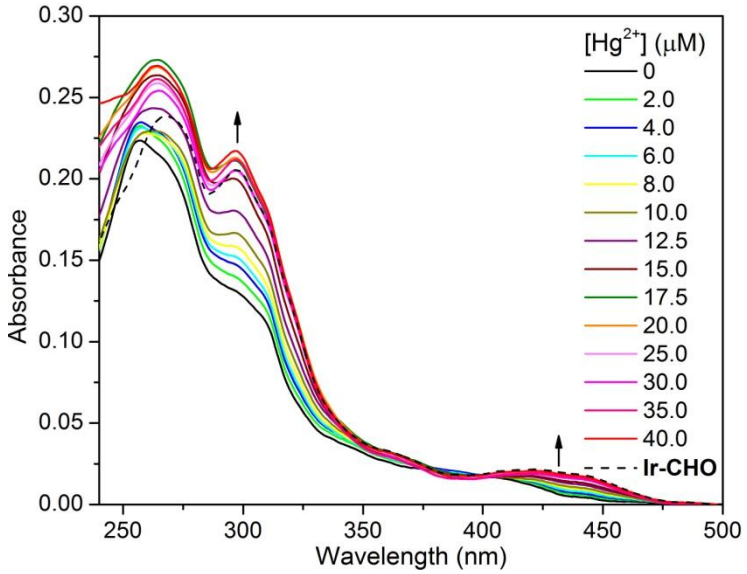

Figure S4. Absorption spectral changes of **Ir-S** (5 μM) in CH_3CN/H_2O (98/2, v/v) upon increasing addition of Hg^{2+} (from 0.0 to 40.0 μM) (perchlorate salt).

6. Luminescent spectral changes of Ir-S upon addition of various metal ions

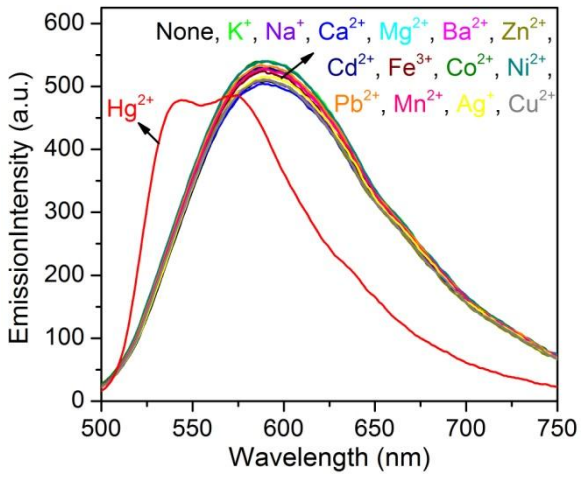

Figure S5. Luminescent response of to **Ir-S** (5 μM) in the absence and presence of various metal ions (perchlorate salts). Hg^{2+} (5 equiv.), other (20 equiv.). CH_3CN/H_2O (98/2, v/v). λ_{ex} = 420 nm.

7. ESI-MS spectral change of Ir-S upon addition of Hg^{2+}

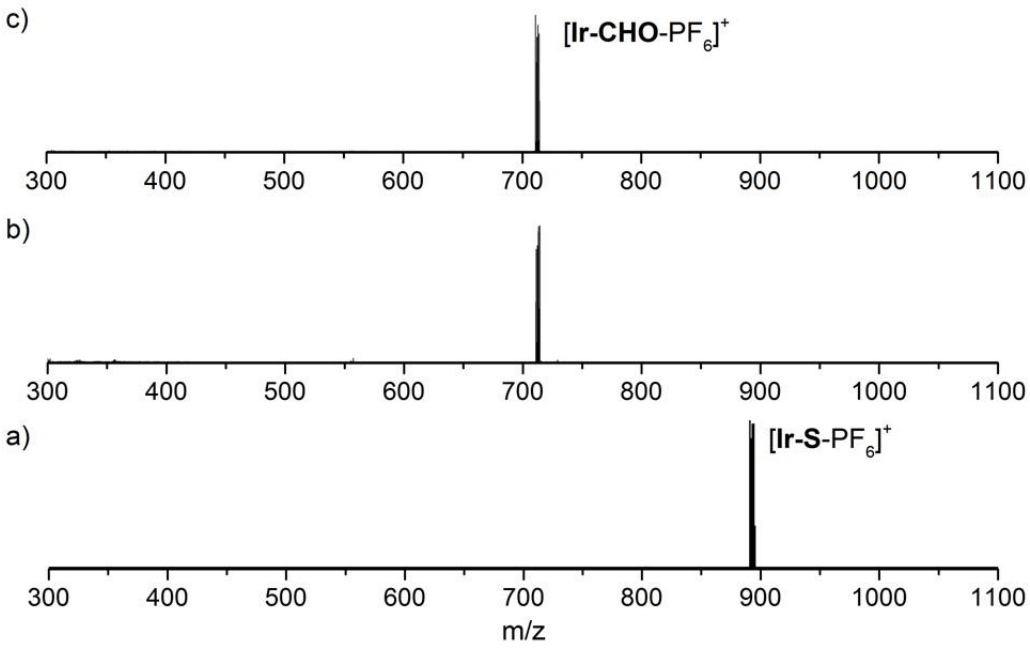

Figure S6. ESI-MS spectra of a) **Ir-S** (10 μM), b) **Ir-S**(10 μM) + 5 equiv. Hg^{2+} and c) **Ir-CHO** (10 μM). CH_3CN/H_2O (98/2, v/v).

8. Optimized structures of Ir-S and Ir-CHO

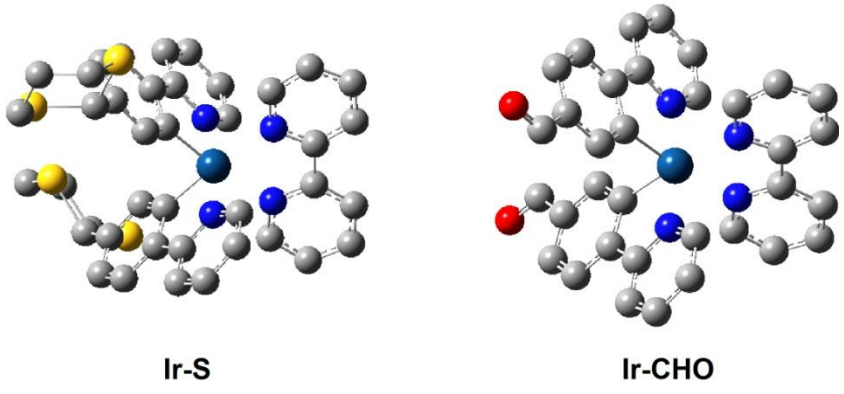

Figure S7. Optimized structure of **Ir-S** and **Ir-CHO** in the ground state (hydrogen atoms are omitted for clarity) with DFT method at the B3LYP level.

9. Experimental and TD-DFT-simulated absorption spectra of Ir-S and Ir-CHO

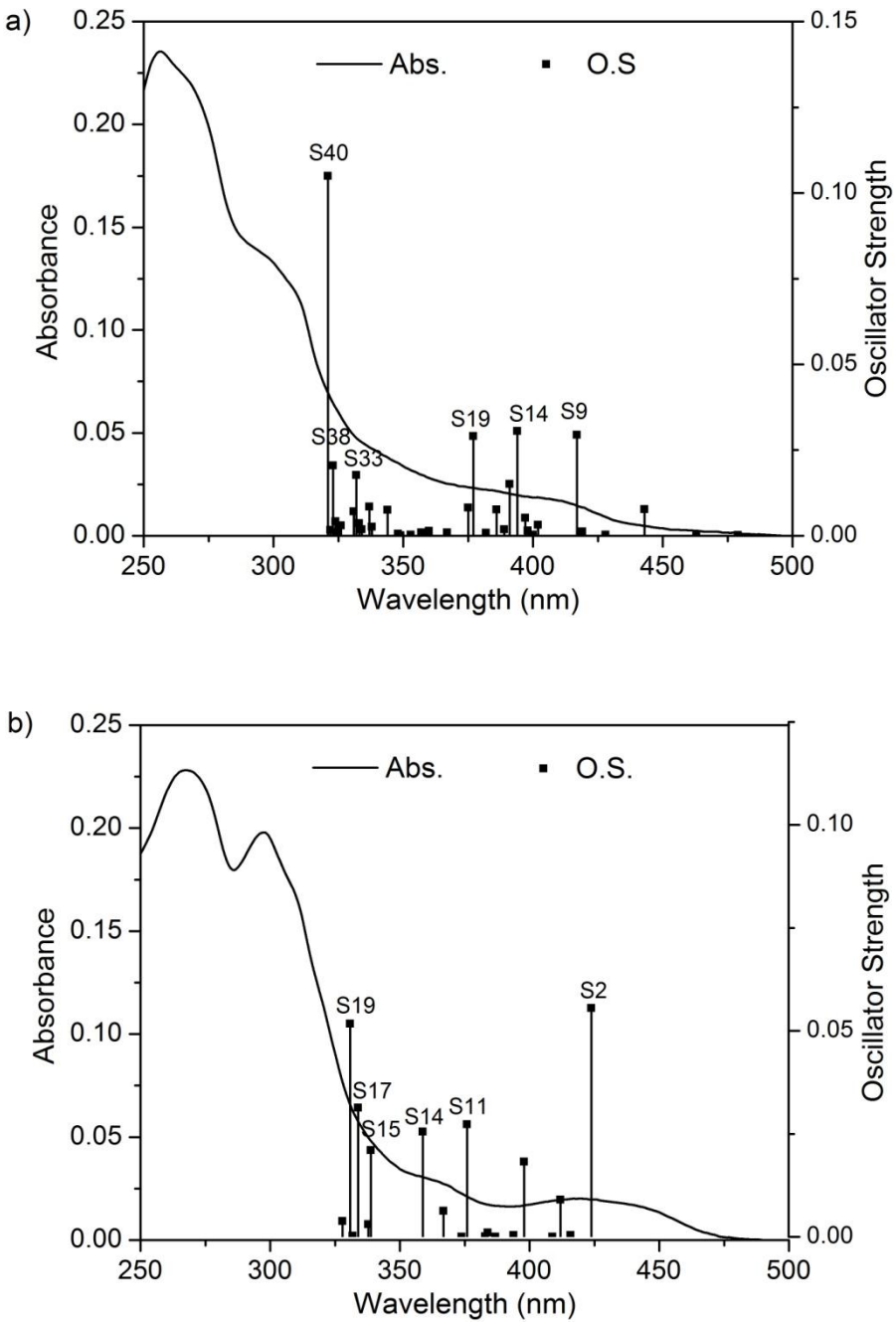

Figure S8. Experimental absorption spectra (line) and TD-DFT-simulated absorption transitions (sticks) of a) **Ir-S** (5 μM), b) **Ir-CHO** (5 μM). CH_3CN.

10. Detailed TD-DFT calculation data of Ir-S

Table S2. Partial molecular orbital compositions of **Ir-S** by the TD-DFT calculations.

Orbital	*E* (eV)	MO contribution (%)							
		Ir	bpy	C^N 1			C^N 2		
				phyridyl	phenyl	dithiane	pyridyl	phenyl	dithiane
LUMO+3	-3.85	3.7	53.5	2.7	1.1	0.2	27.5	9.2	2.1
LUMO+2	-3.96	5.1	3.8	56.3	18.1	3.9	8.2	3.9	0.7
LUMO+1	-4.07	3.2	88.6	3.6	0.9	0.1	2.7	0.9	0.0
LUMO	-4.94	3.9	94.1	0.9	0.1	0.0	0.9	0.1	0.0
HOMO	-7.46	4.4	0.4	0.2	1.3	1.2	0.7	4.8	87.0
HOMO-2	-7.75	34.0	2.9	3.3	16.0	8.4	3.6	18.2	13.6
HOMO-5	-8.26	6.2	1.6	10.2	25.2	3.7	15.1	32.0	6.0
HOMO-6	-8.45	14.9	1.5	10.1	27.9	5.5	5.9	30.5	3.7
HOMO-7	-8.64	14.8	4.4	2.2	41.4	2.4	0.9	32.2	1.7
HOMO-9	-8.84	65.2	6.0	8.0	7.6	1.0	5.8	5.7	0.7

Table S3. Singlet absorption and triplet emission of **Ir-S** by the TD-DFT calculations.

State	Transition	Contri.	*E*, nm (eV)	O.S.	Assignment
T1	HOMO → LUMO	49.0%	606 (2.05)	0.0000	^{3}LLCT
	HOMO-2 → LUMO	40.6%			^{3}LLCT/^{3}MLCT
S9	HOMO → LUMO+2	50.5%	417 (2.97)	0.0294	^{1}LLCT
S14	HOMO-7 → LUMO	54.0%	394 (3.15)	0.0305	^{1}LLCT
S19	HOMO-9 → LUMO	69.4%	377 (3.29)	0.0290	^{1}MLCT
S33	HOMO-5 → LUMO+1	69.6%	332 (3.31)	0.0082	^{1}LLCT
S38	HOMO-6 → LUMO+2	29.8%	323 (3.84)	0.0205	^{1}ILCT/^{1}LLCT
	HOMO-5 → LUMO+3	24.7%			^{1}ILCT/^{1}LLCT
S40	HOMO-5 → LUMO+3	45.3%	321 (3.87)	0.1050	^{1}ILCT/^{1}LLCT

11. Detailed TD-DFT calculation data of Ir-CHO

Table S4. Partial molecular orbital compositions of **Ir-CHO** by the TD-DFT calculations.

Orbital	*E* (eV)	MO contribution (%)				
		Ir	bpy	C^N		
				pyridyl	phenyl	-CHO
LUMO+2	-4.54	4.8	3.6	53.1	26.8	11.7
LUMO+1	-4.64	3.9	3.7	50.2	30.2	12.0
LUMO	-5.32	3.7	94.1	1.8	0.3	0.1
HOMO	-8.23	44.4	3.7	7.5	43.3	1.1
HOMO-2	-8.83	7.6	1.3	15.5	45.3	30.3
HOMO-4	-9.06	19.0	1.3	17.0	51.9	10.8
HOMO-5	-9.17	23.7	4.1	5.7	62.2	4.3
HOMO-6	-9.28	62.8	4.0	13.8	14.3	5.1
HOMO-7	-9.36	57.0	5.4	14.8	19.9	2.9

Table S5. Singlet absorption and triplet emission of **Ir-CHO** by the TD-DFT calculations.

State	Transition	Contri.	*E*, nm (eV)	O.S.	Assignment
T1	HOMO → LUMO	98.8%	563 (2.20)	0.0000	^{3}LLCT/^{3}MLCT
T2	HOMO → LUMO+1	76.4%	500 (2.48)	0.0000	^{3}ILCT/^{3}MLCT
S2	HOMO → LUMO+1	92.0%	424 (2.93)	0.0555	^{1}ILCT/^{1}MLCT
S11	HOMO-5 → LUMO	65.7%	376 (3.30)	0.0273	^{1}LLCT/^{1}MLCT
S14	HOMO-7 → LUMO	79.4%	359 (3.45)	0.0255	^{1}MLCT/^{1}LLCT
S15	HOMO-2 → LUMO+1	61.8%	339 (3.66)	0.0210	^{1}ILCT
S17	HOMO-4 → LUMO+1	35.2%	334 (3.72)	0.0313	^{1}ILCT
	HOMO-6 → LUMO+1	22.1%			^{1}MLCT/^{1}ILCT
S19	HOMO-2 → LUMO+2	68.5%	332 (3.74)	0.0517	^{1}ILCT

12. Calculated molecular orbitals of Ir-S

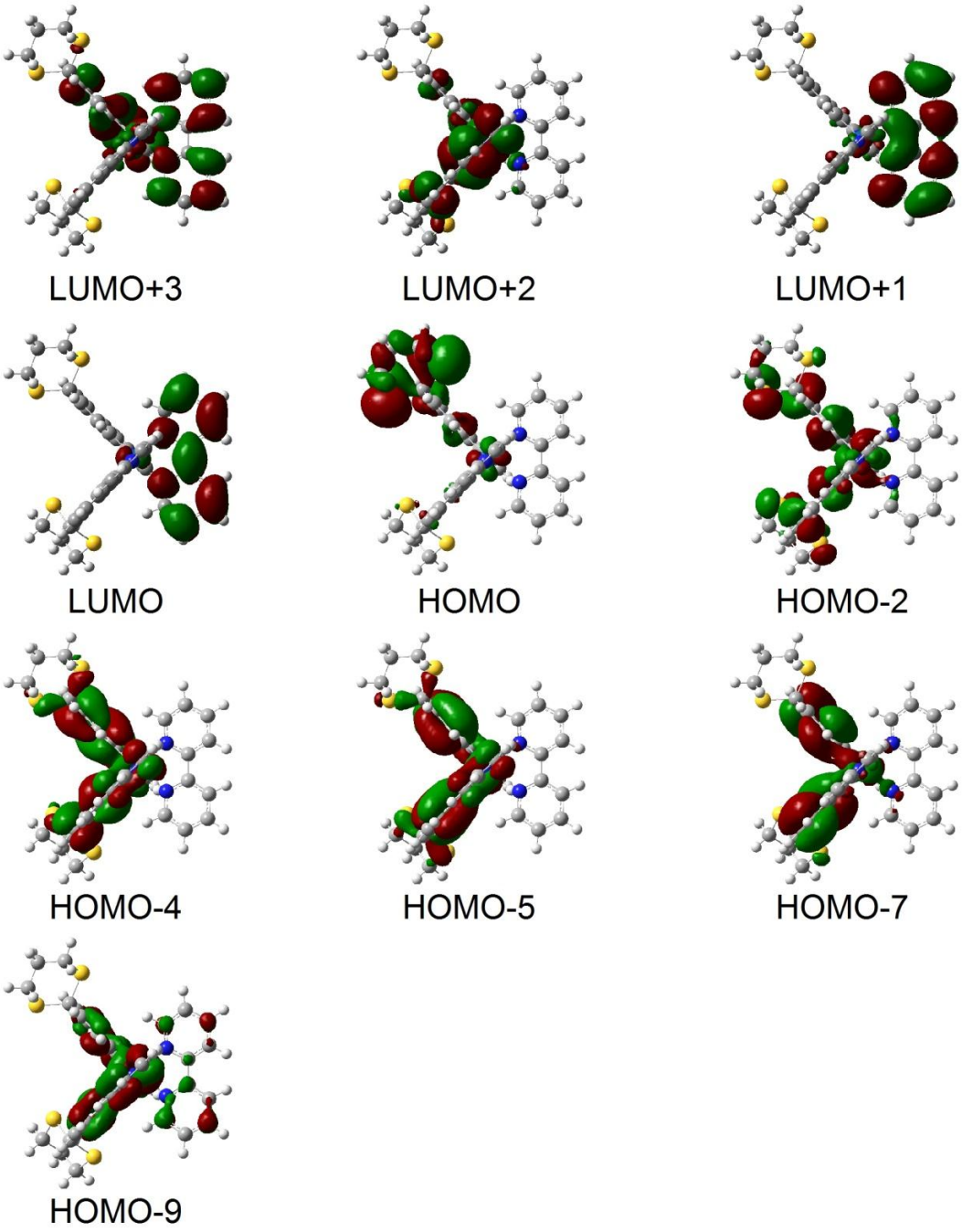

Figure S9. Diagrams of the molecular orbitals involved in the absorption of **Ir-S**.

13. Calculated molecular orbitals of Ir-CHO

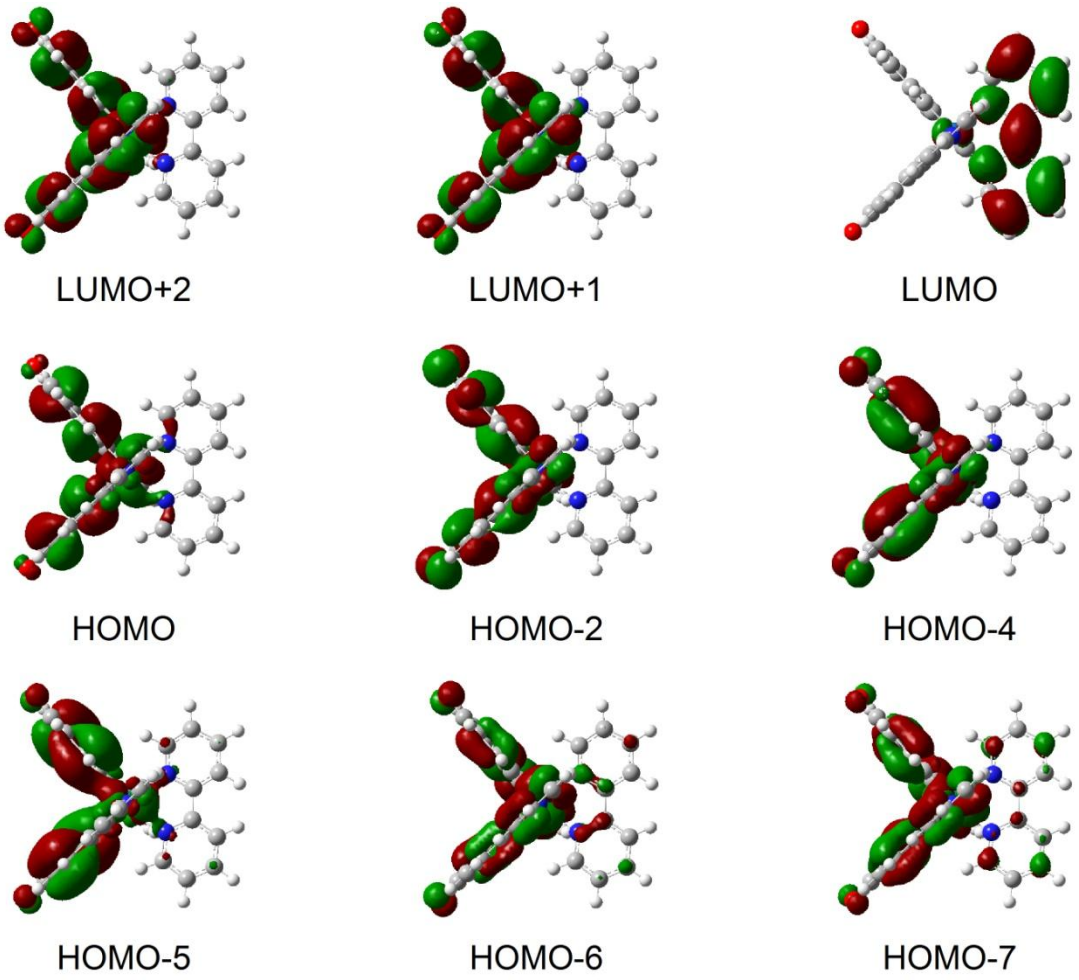

Figure S10. Diagrams of the molecular orbitals involved in the absorption of **Ir-CHO**.

14. ^{1}H NMR, ^{13}C NMR spectra and ESI-MS of Ir-CHO

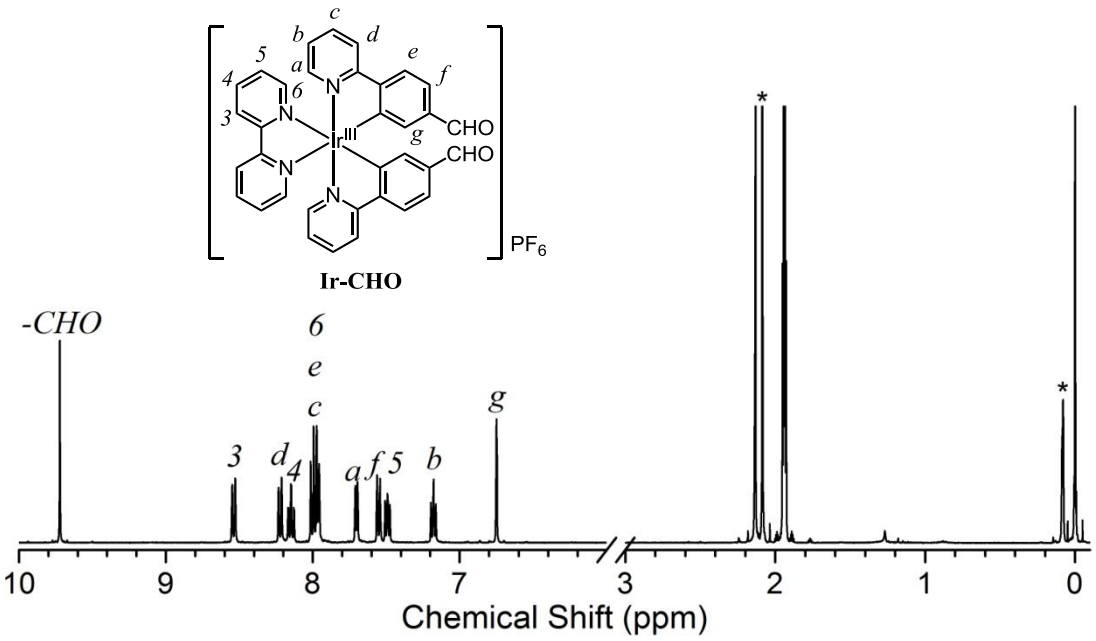

Figure S11. ^{1}H NMR (400 MHz, CD_3CN) spectra of **Ir-CHO**. Asterisks denote residual solvent (2.09 ppm: acetone) and impurity (0.08 ppm) originated from the solvents which were used for recrystallization.

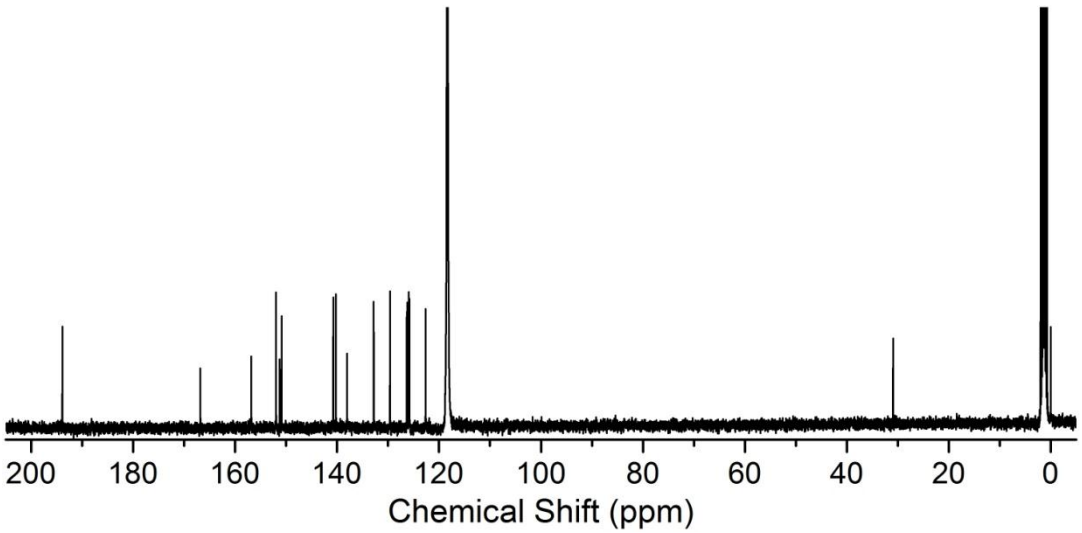

Figure S12. ^{13}C NMR (100 MHz, CD_3CN) spectra of **Ir-CHO**.

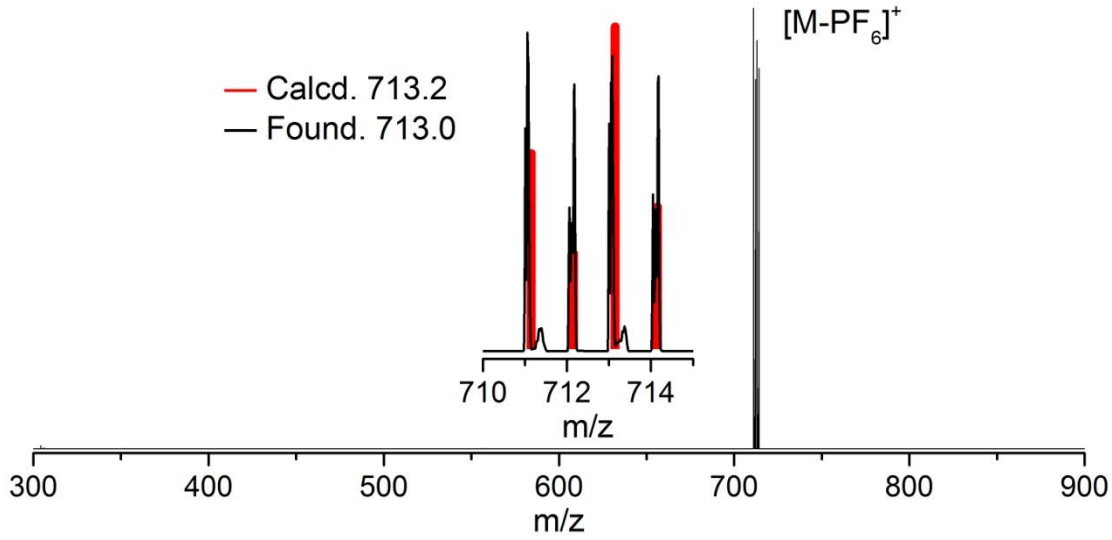

Figure S13. ESI-MS spectra of **Ir-CHO**. CH_3CN.

15. ^{1}H NMR, ^{13}C NMR spectra and ESI-MS of Ir-S

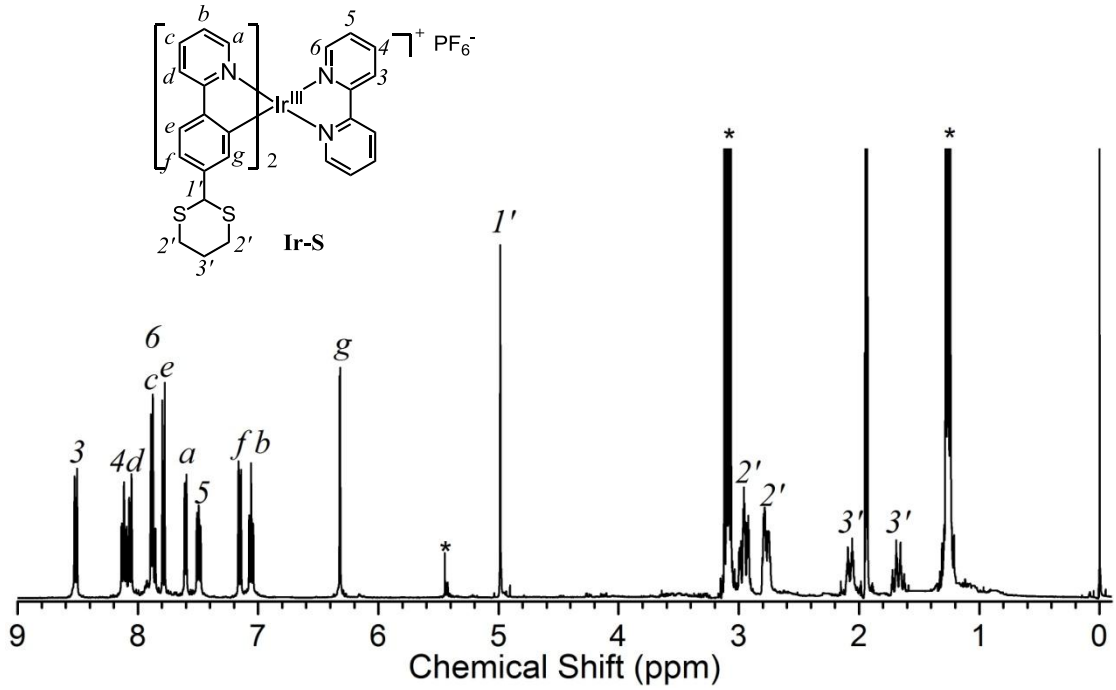

Figure S14. ^{1}H NMR (400 MHz, CD_3CN) spectra of **Ir-S**. Asterisks denote residual solvent (5.44 ppm: CH_2Cl_2) and impurities (3.09 ppm, 1.26 ppm) originated from the solvents which were used for column chromatography.

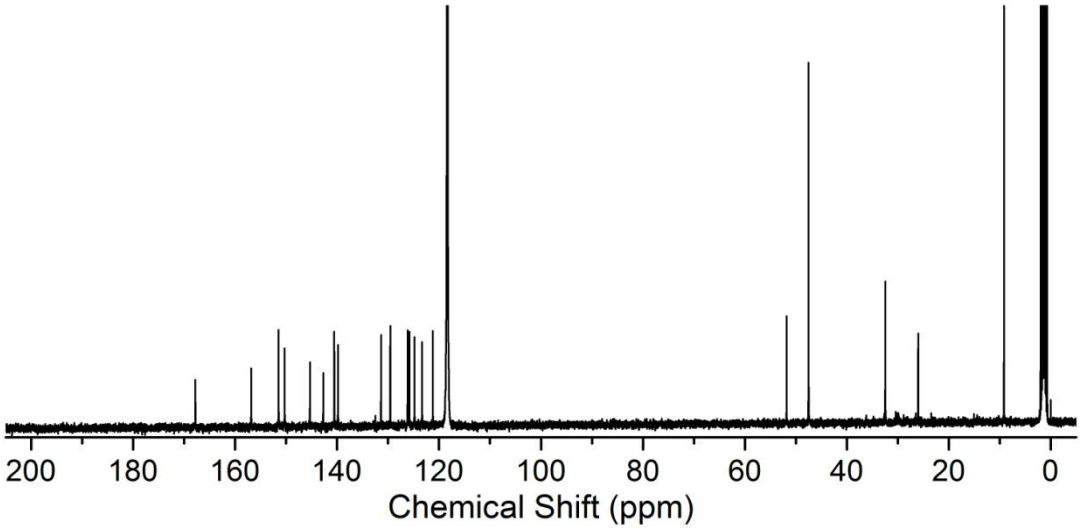

Figure S15. ^{13}C NMR (100 MHz, CD_3CN) spectra of **Ir-S**.

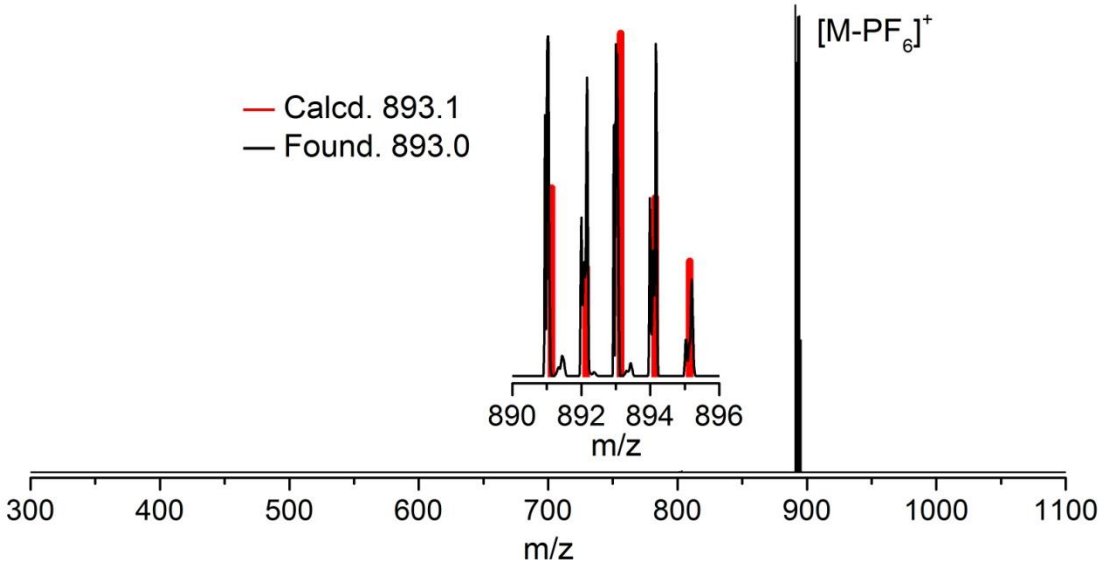

Figure S16. ESI-MS spectra of **Ir-S**. CH_3CN.